REVISTA DE
ENGENHARIA CIVIL IMED

Dynamic thermal behavior and cooling transmission loads of insulated concrete walls under varying environmental conditions for humid subtropical climate

Comportamento térmico dinâmico e cargas de transmissão de resfriamento de paredes de concreto isoladas sob diferentes condições ambientais do clima subtropical úmido

Dimitrios Zenginis(1); Karolos J. Kontoleon(2); Maurício Carvalho Ayres Torres(3)

1 Aristotle University of Thessaloniki, Grécia. E-mail kontoleon@civil.auth.gr
2 Aristotle University of Thessaloniki, Grécia. E-mail: kontoleon@civil.auth.gr
3 Faculdade Meridional IMED, Brasil. E-mail mauricio.torres@imed.edu.br

Revista de Engenharia Civil IMED, Passo Fundo, vol. 5, n. 1, p. 87-101, Jan.-Jun. 2018 - ISSN 2358-6508
[Received: November 21, 2017; Accepted: June 08, 2018]
DOI: https://doi.org/10.18256/2358-6508.2018.v5i1.2288

Evaluation: *Double Blind Review*
Editor-in-chief: Luciana Oliveira Fernandes

Como citar este artigo / How to cite item: clique aqui!/click here!

Abstract

In this study, the effect of insulation thickness and its position on the dynamic thermal characteristics of concrete walls is examined numerically. Regarding the effect of the thermal insulation layer, nine different wall configurations are studied. The analysis is carried out for wall elements with a varying orientation corresponding to each cardinal point for the cooling period and more specifically for the climatic conditions of Thessaloniki, Greece, which climate is classified as Humid Subtropical according to Köppen Climate Classification System, which is the same of Porto Alegre, in Brasil. In addition, diurnal cooling transmission loads are calculated by considering different indoor design temperatures; for the aims of this investigation three typical indoor design temperatures are taken into account (increasing from 24 °C to 28 °C, in steps of 2 °C). Results underline the significance of insulation thickness and position to maintain a stable indoor environment with low temperature fluctuations (decreasing ratio of heat wave temperature amplitudes, decrement factor), as well as to shift adequately the occurred temperature peaks to the inner surface (time delay of heat wave propagation, time lag). It is also seen that north and south oriented walls provide minimum cooling loads compared to walls facing east and west. Furthermore, as the indoor design temperature increases the cooling transmission loads decrease. The thermal performance of insulated concrete walls is studied by using the thermal-network modelling method under steady periodic conditions.

Keywords: Concrete walls. Wall orientations. Insulation thickness/position. Indoor design temperature. Cooling transmission loads.

Resumo

Neste estudo, o efeito da espessura do isolamento e sua posição nas características térmicas dinâmicas das paredes de concreto é examinado numericamente. Quanto ao efeito do isolamento térmico, são estudadas nove diferentes configurações de parede. A análise é realizada para elementos de parede com uma orientação variável correspondente a cada ponto cardinal para o período de resfriamento e mais especificamente para as condições climáticas de Salónica, na Grécia, que tem a mesma classificação climática – subtropical úmido - pelo Sistema Köppen que Porto Alegre, no Rio Grande do Sul, Brasil. Além disso, as cargas de transmissão de resfriamento diurno são calculadas considerando diferentes temperaturas de projeto interno. Para os objetivos desta investigação, são consideradas três temperaturas típicas de design interno (aumentando de 24 °C a 28 °C, em passos de 2 °C). Os resultados sublinham o significado da espessura e posição do isolamento para manter um ambiente interno estável com baixas flutuações de temperatura (proporção decrescente das amplitudes de temperatura da onda de calor, fator de decréscimo), bem como para mudar adequadamente os picos de temperatura ocorridos para a superfície interna (atraso de tempo de propagação de onda de calor, intervalo de tempo). Também é visto que as paredes orientadas norte e sul fornecem cargas de resfriamento mínimas em comparação com as paredes voltadas para o leste e o oeste. Além disso, à medida que a temperatura do projeto interno aumenta, as cargas de transmissão de resfriamento diminuem. O desempenho térmico de paredes de concreto isoladas é estudado usando o método de modelagem de rede térmica em condições periódicas estáveis.

Palavras-chave: Paredes de concreto. Orientação de paredes. Espessura de isolamento. Temperatura de design interior. Cargas de transmissão de refrigeração.

1 Introduction

Worldwide energy consumption has been raising substantially during the last decades because of the fast-economic development, the increasing population and the improving standards of living. This energy is mostly obtained from fossil fuels that stress the greenhouse effect, drive climate changes and empty the fossil fuels supplies rapidly. The building sector (including the building industry sector) is considered to be globally the main world energy consumption contributor (UNITED NATIONS ENVIRONMENT PROGRAMME, 2009). With reference to Europe, residential and commercial buildings require around 40% of the overall energy use (EUROPEAN COMMISSION, 2016). Thus, it is clear that actions and interventions that improve the thermal and energy performance of buildings will decisively benefit energy usage globally.

The determination of time lag and decrement factor play a pivotal role in obtaining the dynamic thermal characterization of building envelopes. The study of these dynamic thermal characteristics of buildings is receiving great interest. Asan (2000) investigated the wall's optimum insulation position from the maximum time lag and minimum decrement factor point of view by employing the *Crank – Nicolson* methodology under periodic convection boundary conditions on both exterior and interior boundaries. Ozel (2014) assessed numerically the influence of the thermal insulation location and thickness on the thermal inertia parameters of building walls by using an implicit finite difference method under steady periodic conditions. Kontoleon and Eumorfopoulou (2008) examined the effect of wall orientation and exterior surface solar absorptivity on time lag and decrement factor values using the thermal network model. In another study, the unsteady thermal response parameters of a building roof have been investigated by solving a one-dimensional diffusion equation under convective periodic boundary conditions (SHAIK; TALANKI, 2016).

In addition, several studies deal with the calculation of the heating and cooling transmission loads in buildings that is an essential step for a successful sizing of an HVAC system. For instance, Ozel (2016) determined numerically the impact of indoor design temperatures on both cooling and heating transmission loads through walls with different orientations. Al-Sanea et al. (2016) estimated yearly transmission loads for various wall configurations by utilizing a validated computer model based on the finite-volume implicit method. Pegdogan and Basaran (2017) analyzed numerically the heat transfer through external wall structures based on insulation position and wall orientation. More recently, the effects of adding phase change materials to single and multilayer building envelopes on their thermal performance has been presented by evaluating the dynamic thermal characteristics and the heating and cooling transmission loads. (MAZZEO et al., 2017; SHARIFI et al., 2017; THIELE et al., 2017).

In this study, the thermal behavior of insulated concrete walls is extensively examined for summer conditions and northern, eastern, southern and western

orientations. Meteorological data corresponding to the city of Thessaloniki in northern Greece were used in these calculations. In first step, different insulation positions and thicknesses are taken into account in order to evaluate the time lag and decrement factor. Then, using the same wall configurations, three typical indoor design temperatures are considered in order to estimate daily cooling transmission loads. It is important to underline that the utilization of the thermal mass with regard to opaque building elements is essential in order to attain desirable thermal comfort conditions (passive buildings) or to decrease the energy demands (buildings with *HVAC* units). In particular, for building envelopes subjected to cyclic ambient variations in temperature, such as those exposed during the summer period in the Greek region, the contribution of the indoor design temperature on their thermal performance is significant. In order to accomplish the transient thermal analysis, a proper one-dimensional thermal-network model is employed.

2 Methodology

2.1 Thermal-network modelling and transient analysis

In this investigation a lumped capacitance thermal-network model that incorporates a single heat flow path is employed. This path corresponds to one-dimensional conduction-dominated transient heat transfer prevailed in the direction perpendicular to the building envelope surface (the heat transfer in the *y*-direction and *z*-direction is assumed to be negligible). Moreover, the model simulates combined convective and radiative heat transfer processes on both boundaries of the building envelope by assuming: (a) a periodic sol-air temperature T_{sa} forcing function imposed at the exterior wall surface and (b) a constant indoor temperature T_{in} forcing function at the interior wall surface. The heat flow path includes a discrete number of *RC*-sections (*R* refers to thermal resistances, while *C* refers to thermal capacitances). Each *RC*-section of a layer *n* contains two resistances R_n and a single lumped capacitance C_n at the mid-node. The values of *R* and *C* depend on the area, the thicknesses and thermophysical properties of building material layers. The *RC*-section layers comprising the wall formations are connected to T_{sa} and T_{in} temperature sources with the heat transfer resistances R_e and R_i (CENGEL, 2003):

$$R_e = \frac{1}{h_e}\ [\mathrm{m^2 \cdot K \cdot W^{-1}}] \quad \text{and} \quad R_i = \frac{1}{h_i}\ [\mathrm{m^2 \cdot K \cdot W^{-1}}] \tag{1}$$

where h_e and h_i are the heat transfer coefficients due to combined convection and radiation on the outer and the inner surface of the wall, respectively. The modelling of a heat flow path, based on the thermal-network methodology, is depicted in Fig. 1.

Fig. 1. Thermal analysis through a multilayered element by means of the thermal-network approach

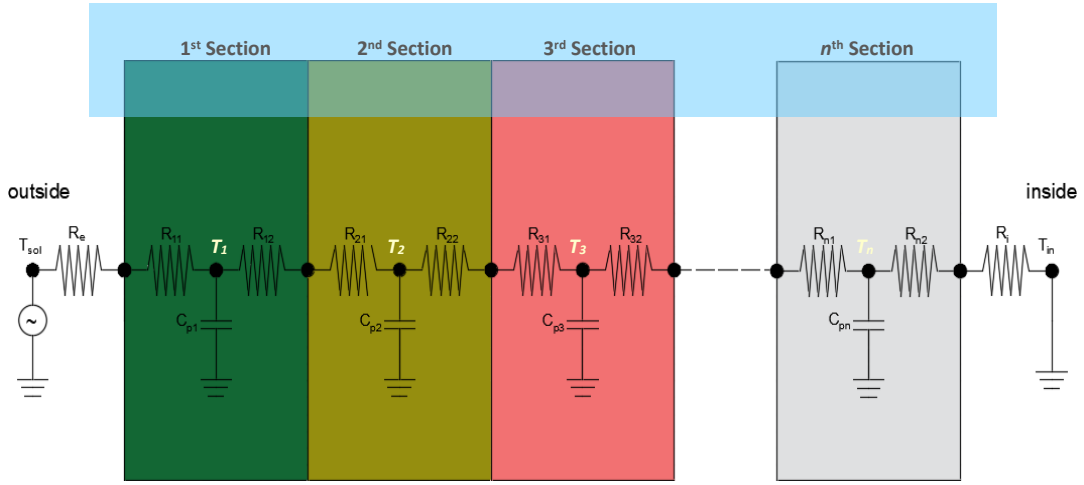

The adopted solution provides the wall outer and inner surface temperatures and the temperature of any location at any time of the day. Thus, the dynamic thermal characteristics and the daily transmission loads are computing as following.

The time lag φ is defined as follows:

$$\varphi=\begin{cases} t_{T_i}^{max} > t_{T_e}^{max} \Longrightarrow t_{T_i}^{max} - t_{T_e}^{max} \\ t_{T_i}^{max} < t_{T_e}^{max} \Longrightarrow t_{T_i}^{max} - t_{T_e}^{max} + P \quad [h] \\ t_{T_i}^{max} = t_{T_e}^{max} \Longrightarrow P \end{cases} \tag{2}$$

where t_{Ti}^{max} and t_{Te}^{max} represent the time (in hours) when inside and outside surface temperatures reach their respective maximum and P (24-h) is the period of the temperature oscillation.

Moreover, the decrement factor f (dimensionless characteristic) is defined as:

$$f=\frac{A_i}{A_e}=\frac{T_i^{max}-T_i^{min}}{T_e^{max}-T_e^{min}} \quad [-] \tag{3}$$

where A_i and A_e are the amplitudes of oscillation in temperature at the inner and outer surfaces of a wall, respectively.

The instantaneous transmission heat load is obtained as:

$$q_i(t)=h_i \cdot (T_i(t) - T_{in}) \quad [W \cdot m^{-2}] \tag{4}$$

In order to calculate the daily total load, this instantaneous load is integrated over the 24-hour period.

2.2 Description of analyzed wall configurations and environmental conditions

The goal of this study was to stress general trends regarding the influence of insulation thickness and position and indoor temperature on the dynamic thermal characteristics and cooling transmission loads, respectively. In this context, architectural features such as windows and doors were not considered. The investigation is carried out for multilayer building envelopes consisting of light weighted plaster (coatings) of thickness d_{LWP} = 1 cm on both surfaces, concrete wall (masonry layer/layers, **M**) of thickness d_{CON} = 25 cm as one layer and d_{CON} = 12.5 cm as two equivalent sections and extruded polystyrene (XPS thermal insulation layer, **I**) with a varying thicknesses. For the aims of this study three thicknesses of the thermal insulation layer are considered d_{XPS} = 6 cm, d_{XPS} = 9 cm and d_{XPS} = 12 cm . The thermal insulation layer is placed on the outer surface, the inner surface and the mid-center of the concrete wall. Thus, the analysed wall assemblies are denoted as **IM**, **MI** and **MIM**, respectively (Fig. 2). In overall, based on the location and widths of the thermal insulation layer the amount of the studied walls is equal to nine. Furthermore, the examined building elements are considered to have an orientation that corresponds to all cardinal points (north, east, south and west). Table 1 depicts the thicknesses d and the thermophysical properties k, ρ, C_p of the examined building materials considered in this work.

Fig. 2. Investigated building envelope configurations including a thermal insulation layer at: (a) the outer surface – **IM** configuration, (b) the inner surface – **MI** configuration, (c) the mid-center of the masonry layer – **MIM** configuration.

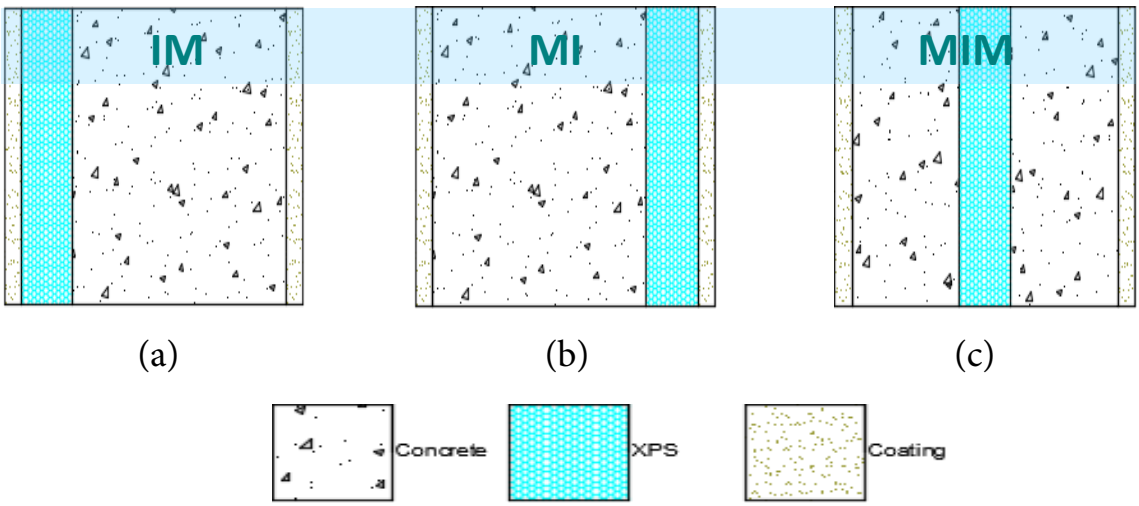

Table 1 – Geometrical characteristics and thermophysical properties of building materials

Material Name	d **[cm]**	k **[W·m^{-1}·K^{-1}]**	**ρ [kg·m^{-3}]**	C_p **[J·kg·K^{-1}]**
Reinforced concrete	25	2.50	855	1000
Extruded polystyrene XPS	6, 9, 12	0.03	35	1200
Light weighted plaster	1	0.87	1800	1100

With regard to the external environmental conditions, the aforementioned building configurations are subjected to a realistic sol-air temperature for a representative day of July (16th of July) in mild Mediterranean climate (Greek region) and for a latitude 40^{o} 38' N (Thessaloniki). The sol-air temperature T_{sa} accounts for the thermal effects of actual ambient-air temperature and incident solar radiation flux on the outer surface of the building envelopes and is defined as:

$$T_{sa}(t)=T_o+\frac{\alpha_{sol}\cdot q_{sol}}{h_e}\ [^{o}C] \quad (5)$$

where T_o is the outdoor air temperature, q_{sol} and α_{sol} denote the solar radiation heat flux and solar absorptivity of the outdoor wall surface, respectively, and h_e is the outer heat transfer coefficient, due to combined convection and radiation, defined in Eq. (1). The outdoor air temperatures in Thessaloniki are obtained from the National Meteorological Service, while the solar radiation flux on the wall is calculated by using the *ASHRAE clear-sky model*. The solar absorptivity of the opaque building envelope was taken to be α_{sol} = 0.25 and the combined heat transfer coefficient at the exterior surface equal to h_e = 25 W·m^{-2}·K^{-1} (TECHNICAL CHAMBER OF GREECE, 2010). Hourly variations of sol-air temperature and incident solar radiation of external opaque surfaces in July 16 are shown in Fig. 3 (a) and (b), respectively. Conversely, the indoor air temperature T_{in} is presumed to be constant in the time domain; its value ranged between T_{in} = 24 °C and T_{in} = 28 °C, in steps of 2 °C. The combined heat transfer coefficient at the interior surface of the facade is taken to be h_i = 7.69 W·m^{-2}·K^{-1} (TECHNICAL CHAMBER OF GREECE, 2010). Evidently, thermophysical properties of involved building materials where considered to be unvarying for the assumed environmental conditions.

Fig. 3. Hourly variations of (a) sol-air temperature T_{sa} and (b) incident solar radiation q_{sol} for all building envelope orientations in July 16.

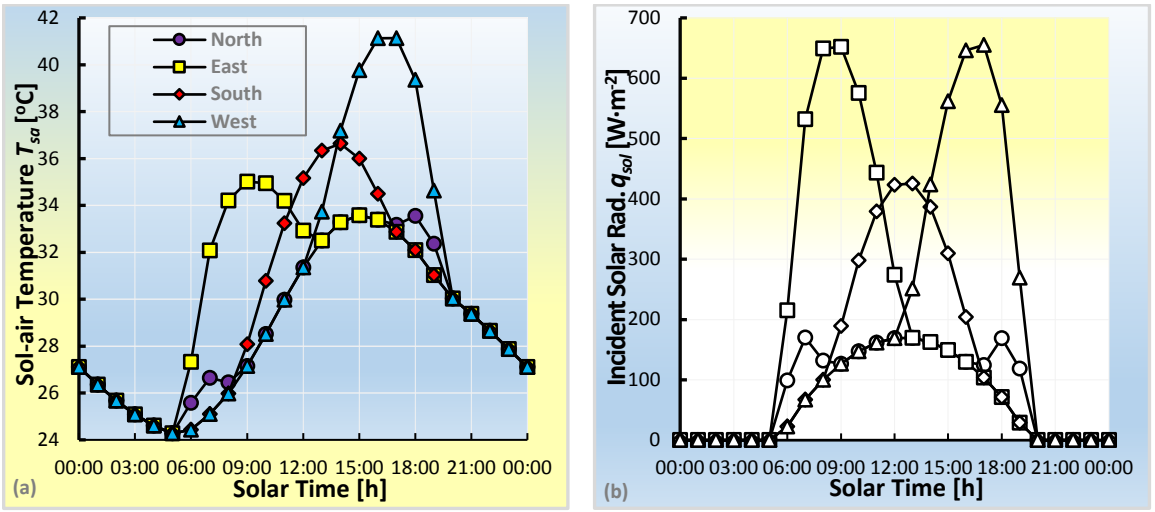

3 Results and discussion

3.1 Time lag and decrement factor trends

In this section, results of the thermal inertia parameters, time lag and decrement factor, are discussed in terms of insulation thickness and position. The analyses were conducted for a representative day of July (16th of July) for all the compass point orientations, while the value of the forced room air-temperature was assumed to be equal to T_{in} = 26 °C.

3.1.1 Time lag fluctuations

As seen from the graphs in Fig. 4 (a)-(d), the insulation thickness influence is substantial. As the thickness of the insulation increases, the time lag increases for all orientations and the three positions of the insulation material. For example, for east orientation, when the insulation is placed on the outer surface of the concrete wall $\varphi_{d\text{-}XPS=6cm}$ = 12.66 h, $\varphi_{d\text{-}XPS=9cm}$ = 13.08 h and $\varphi_{dXPS=12cm}$ = 13.5 h. It is mentioned that the variation of φ values with the thickness of the thermal insulation layer d_{XPS} shows an almost linear trend, which agrees with several previous studies (Asan 1998; Ozel 2014).

As for the influence of insulation position, this highly depends on the building envelope orientation. As shown in Fig. 4 (a)-(b), for north and east oriented building envelopes, the placement of insulation on the outer surface (IM wall) of the concrete wall leads to the maximum time lag values; for d_{XPS} = 9 cm, φ_{IM} = 9.25 h and φ_{IM} = 13.08 h, respectively. However, a discrepancy is observed regarding the minimum values of time lag. More specifically, a north/east orientation shows the minimum value when the insulation is placed on the inner surface (MI wall) / the mid-center (MIM

wall) of the concrete wall, with a value of φ_{MI} = 6.25 h / φ_{MIM} = 8.75 h, for d_{XPS} = 9 cm, respectively. On the other hand, as shown in Fig. 4 (c)-(d), for south and west oriented building elements, the maximum time lag values are noticed when the insulation is located at the mid-center (MIM wall) of the concrete wall, whereas the minimum ones are presented when the insulation is assumed to be placed on the inner surface (MI wall); for d_{XPS} = 9 cm, the respective values are φ_{MIM} = 11 h, φ_{MI} = 9 h (south orientation) and φ_{MIM} = 8.58 h, φ_{MI} = 6.41 h (west orientation).

Fig. 4. Time lag φ for building envelopes with different insulation positions and thicknesses and for a (a) north, (b) east, (c) south and (d) west orientation

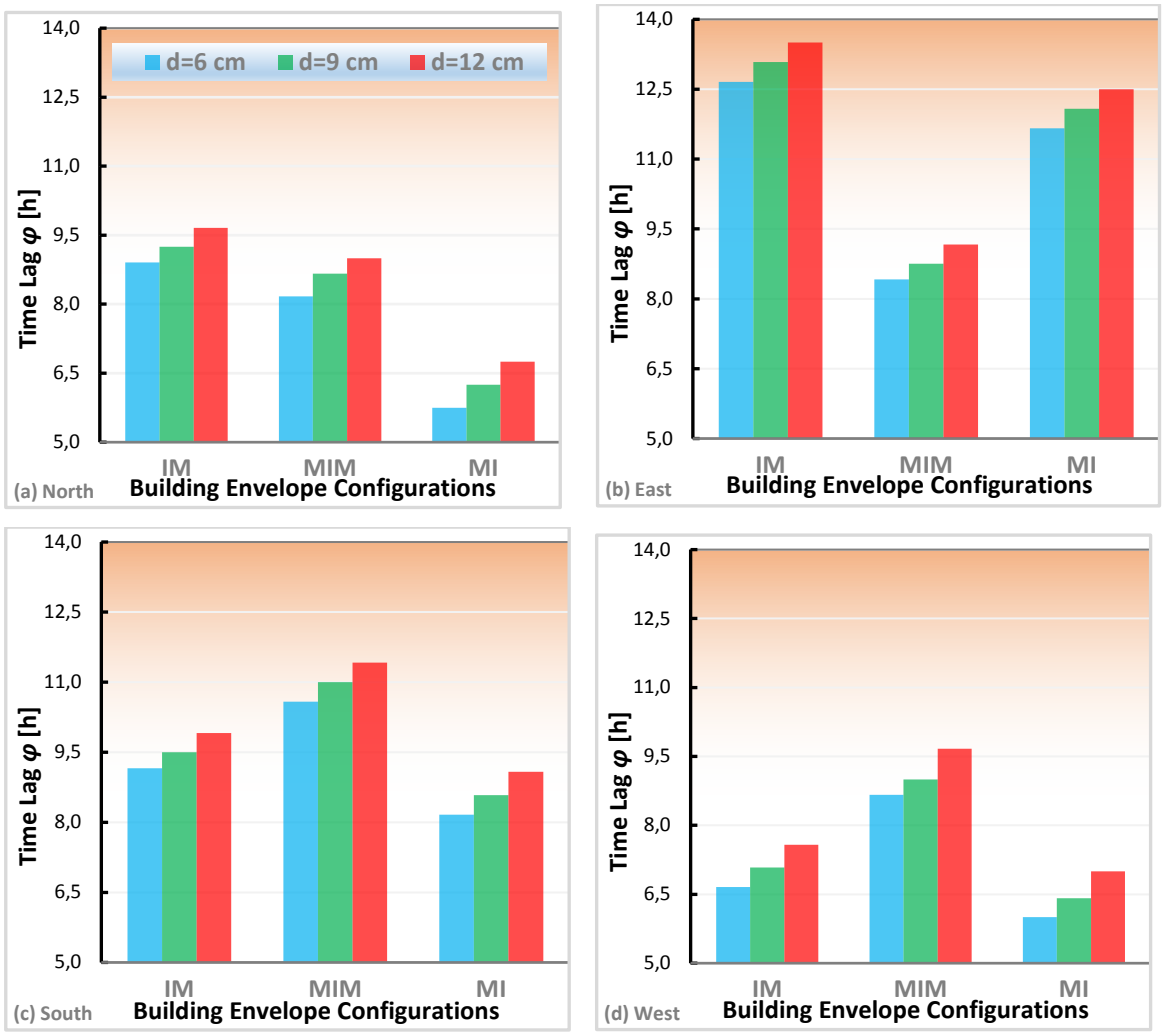

3.1.2 Decrement factor fluctuations

The column bars on Fig. 5 (a)-(d) demonstrate the effect of insulation thickness and position on the decrement factor.

From an overall perspective, it is clear that the effect of insulation material thickness is significant, as an increase in insulation thickness leads to a parallel decrease in the decrement factor value regardless of the orientation and the insulation

position. For instance, for an east oriented wall, when the insulation is placed on the outer surface (IM wall) of the concrete wall $f_{d\text{-}XPS=6cm}$ = 0.0062, $f_{d\text{-}XPS=9cm}$ = 0.0041 and $f_{d\text{-}XPS=12cm}$ = 0.0030. It is also important to mention that as the insulation thickness increases the decrease trend on *f* values shows a lessening.

In terms of the results of the effect of insulation position on the decrement factor, the same trend is followed for all orientations. In particular, when the insulation material is placed on the outer surface of the concrete wall then the minimum decrement factor values occur, while when it is placed on the inner one the decrement factor values are the maximum ones. The location of insulation at the mid-center of the concrete wall provides an intermediate value for all wall orientations. For example, for a north oriented building envelope and d_{XPS} = 9 cm, the respective values are f_{IM} = 0.0045, f_{MI} = 0.0133 and f_{MIM} = 0.0081. Likewise, for a south oriented building zone and for d_{XPS} = 9 cm the *f* values are f_{IM} = 0.0043, f_{MI} = 0.0135 and f_{MIM} = 0.0067, respectively.

In addition, when the orientation of a wall element is examined the differences among the *f* values is shown to be negligible. For an insulation layer of thickness d_{XPS} = 6 cm positioned on the inner surface of a wall (MI wall) the decrement factor values for a north, an east, a south and a west assembly are 0.0195, 0.0197, 0.0199 and 0.0186, respectively. Furthermore, for d_{XPS} = 12 cm and for all analysed cardinal wall orientations the *f* values coincide (f ≈ 0.0100).

3.2 Cooling transmission loads

In this subsection, cooling transmission loads are calculated for different building envelope orientations as indoor design temperature is increasing from T_{in} = 24 °C to T_{in} = 28 °C in steps of 2 °C and insulation thickness is increasing from d_{XPS} = 6 cm to 12 cm, in steps of 3 cm. The insulation material is assumed to be placed on the outer surface of the concrete wall (designated as IM wall configuration).

It is obvious that adopting a more moderate design for the increase of indoor temperature settings marks a considerable decline in cooling transmission loads. The results show that for all insulation thicknesses reduction in cooling loads for north, east/west and south is obtained to be approximately 80%, 63% and 70%, respectively.

Furthermore, it is evident that east/west orientations give the maximum values of cooling loads of about 50 - 240 kJ/m^2, whereas north and south orientation have lower ones of about 20 - 190 kJ/m^2 and 30 - 210 kJ/m^2 respectively. This is due to the variation in the amount of solar radiation received by these surfaces; during the cooling period the values of the incoming solar radiation for east/west surfaces are sharply higher compared to those for north and south surfaces. The amount of solar radiation received by east oriented building envelopes is equal to that received by the west ones. Therefore, the resulting cooling transmission loads for these orientations are also equal and are presented in the same graph.

Fig. 5. Decrement factor *f* for building envelopes with different insulation positions and thicknesses and for a (a) north, (b) east, (c) south and (d) west orientation

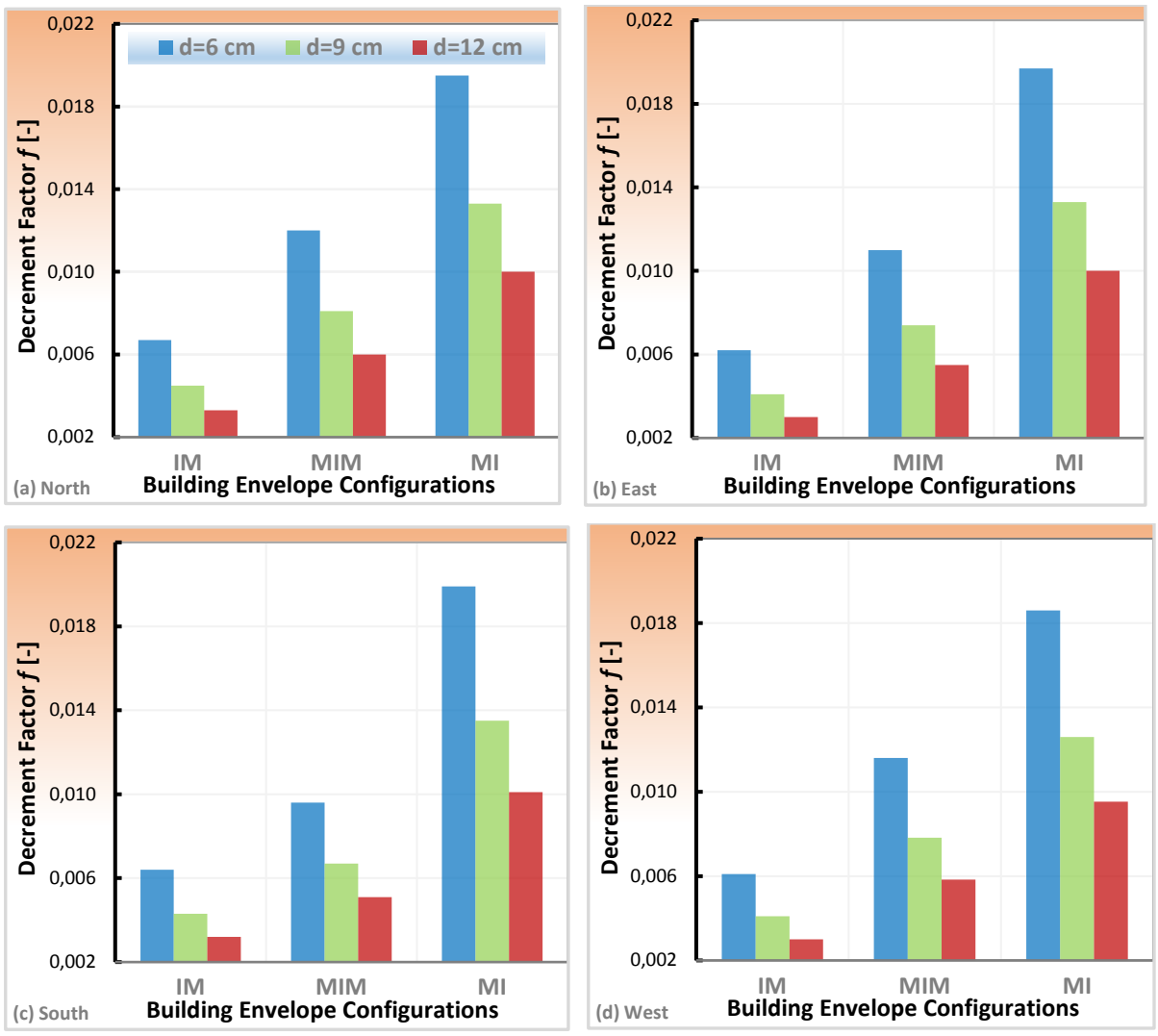

The influence of the insulation layer thickness on the occurring cooling loads is shown in Fig.6 (a) – (c). An increase in the insulation layer thickness results in a major decrease in cooling transmission loads for all assumed indoor temperature settings.

Fig. 6. Cooling transmission loads for the 16th of July with respect to different insulation thicknesses and indoor design temperatures for (a) north, (b) east/west and (c) south oriented building envelopes

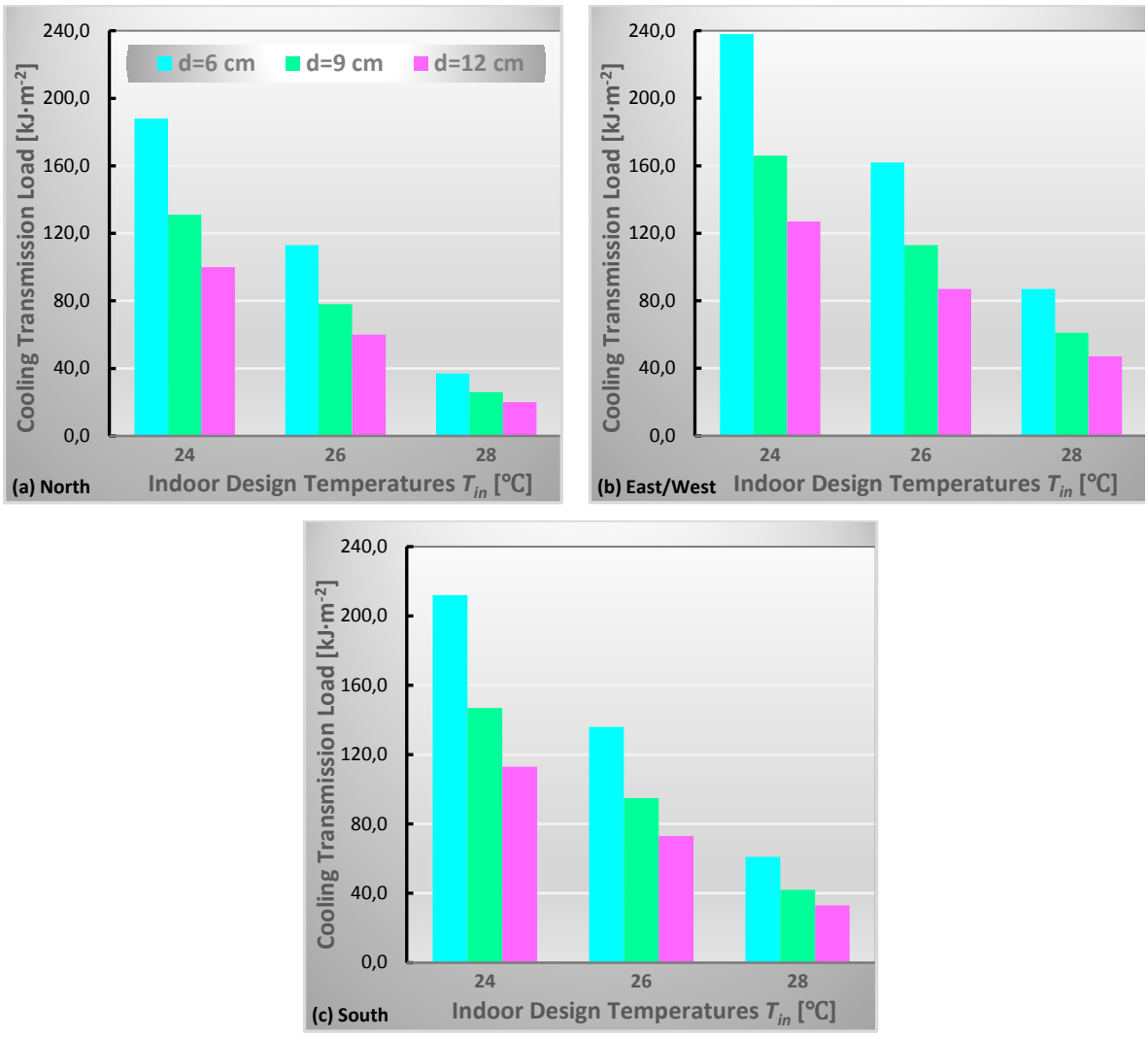

4 Conclusions

The present study analysed the effect of insulation thickness and position on the dynamic thermal characteristics of concrete wall assemblies as well as the impact of the selected indoor design temperatures on the cooling transmission loads through them. The investigation has been carried out for different wall configurations and orientations in the climatological conditions of Thessaloniki, Greece, by employing a lumped thermal-network model.

The obtained results of this study underline the importance of thermal insulation location and thickness on both thermal inertia parameters (time lag and decrement factor). The combined effect of thermal insulation characteristics as well as the orientation of wall assemblies was shown to be influential to attain the highest delay

of the heat wave propagation and to reduce the ratio of the internal amplitude of the temperature oscillation to the external one. It was revealed that by increasing the insulation thickness the thermal performance of a wall can be essentially improved, and thus, the time lag rises, and the decrement factor declines. From the point of view of the selection of the indoor design temperatures that affect the occurring cooling transmission loads, it was determined that a stricter design aiming to the decrease of indoor temperature settings can result in a larger rise of cooling loads.

References

AL-SANEA, S.A.; ZEDAN, M.F.; AL-MUJAHID, A.M.; AL-SUHAIBANI, Z.A. Optimum R-values of building walls under different climatic conditions in the Kingdom of Saudi Arabia. *Applied Thermal Engineering*, v. 96, p. 92-106, 2016. doi: https://doi.org/10.1016/j.applthermaleng.2015.11.072

ASAN, H. Effects of wall's insulation thickness and position on time lag and decrement factor. *Energy and Building*, v. 28, n. 3, p. 299-305, 1998. doi: https://doi.org/10.1016/S0378-7788(98)00030-9

ASAN, H. Investigation of wall's optimum insulation position from maximum time lag and minimum decrement factor point of view. *Energy and Building*, v. 32, n. 2, p. 197-203, 2000. doi: https://doi.org/10.1016/S0378-7788(00)00044-X

ÇENGEL, Y.A. *Heat Transfer*: A Practical Approach. Mc Graw-Hill, 2003.

EUROPEAN COMMISSION. Directive 2010/31/EU of the European parliament and the council of 30 November 2016 on the energy performance of buildings. 2016.

KONTOLEON, K.J.; EUMORFOPOULOU, E.A. The influence of wall orientation and exterior surface solar absorptivity on time lag and decrement factor in the Greek region. *Renewable Energy*, v. 33, n. 7, p. 1652-1664, 2008. doi: https://doi.org/10.1016/j.renene.2007.09.008

MAZZEO, D.; OLIVETI, G.; ARCURI, N. Definition of a new set of parameters for the dynamic thermal characterization of PCM layers in the presence of one or more liquid-solid interfaces. *Energy and Buildings*, v. 141, p. 379-396, 2017. doi: https://doi.org/10.1016/j.enbuild.2017.02.027

OZEL, M. Effect of insulation location on dynamic heat-transfer characteristics of building external walls and optimization of insulation thickness. *Energy and Buildings,* v. 72, p. 288-295, 2014. doi: https://doi.org/10.1016/j.enbuild.2013.11.015

OZEL, M. Effect of indoor design temperature on the heating and cooling transmission loads. *Journal of Building Engineering*, v. 7, p. 46-52, 2016. doi: https://doi.org/10.1016/j.jobe.2016.05.001

PEKDOGAN, T.; BASARAN, T. Thermal performance of different exterior wall structures based on wall orientation. *Applied Thermal Engineering*, v. 112, p. 15-24, 2017. doi: https://doi.org/10.1016/j.applthermaleng.2016.10.068

SHAIK, S.; TALANKI, A.B.P.S. Optimizing the position of insulating materials in flat roofs exposed to sunshine to gain minimum heat into buildings under periodic heat transfer conditions. *Environmental Science and Pollution Research*, v. 23, n. 10, p. 9334-9344, 2016. doi: https://doi.org/10.1007/s11356-015-5316-7

SHARIFI, N.P.; SHAIKH, A.A.N.; SAKULICH, A.R. Application of phase change materials in gypsum boards to meet building energy conservation goals. *Energy and Buildings*, v. 138, p. 455-467, 2017. doi: https://doi.org/10.1016/j.enbuild.2016.12.046

TECHNICAL CHAMBER OF GREECE. Energy Performance of Buildings Directive - Technical Guidelines - T.O.T.E.E. 20701-1/2010 - Guidelines on the evaluation of the energy performance of buildings. 2010.

THIELE, A.M.; LIGGET, R.S.; SANT, G.; PILON, L. Simple thermal evaluation of building envelopes containing phase change materials using a modified admittance method. *Energy and Buildings*, v. 145, p. 238-250, 2017. doi: https://doi.org/10.1016/j.enbuild.2017.03.046

UNITED NATIONS ENVIRONMENT PROGRAMME. Buildings and Climate Change: summary for decision makers. Sustainable Buildings and Climate Initiative, United Nations Environmental Programme, 2009. doi: https://doi.org/10.1007/978-1-4471-4781-7_2